Astronomy & Astrophysics

Polarization of radiation scattered in magnetized turbulent envelopes

N. A. Silant'ev[1,2]

[1] Instituto Nacional de Astrofísica, Óptica y Electrónica, Apartado Postal 51 y 216, CP 72000, Pue. México
e-mail: silant@inaoep.mx

[2] Main Astronomical Observatory of the Russian Academy of Sciences, Pulkovo, St.Petersburg 196140, Russia

ABSTRACT

We consider the single scattering of the non-polarized radiation of a central star on the electrons of a plasma circumstellar envelope. We assume that such an envelope is magnetized and consists of a turbulent plasma. Two types of envelopes are considered: a spherical envelope with the dipole magnetic field and a cone-like jet with the radial magnetic field. It is shown that the existence of turbulent motions in the envelopes drastically changes the polarization degree spectrum $p(\lambda)$ and the positional angle spectrum $\chi(\lambda)$ of scattered radiation compared to the non-turbulent case. The difference in spectra can be used to estimate the ratio for the energy of magnetic fluctuations to the energy of a regular magnetic field.

Key words. polarization – magnetic fields

1. Introduction

There are a lot of observational data on the existence of stellar winds, jets, and envelopes for various stars, quasars, and active galactic nuclei (see for example, Hartmann 1983; Impey et al. 1991; Landstreet 1992; Wills et al. 1992; Paatz & Camenzind 1996). Many of these envelopes possess magnetic fields (see recent observations of Udompraset et al. 1997; Ishwara-Chandra et al. 1998; Pentericci et al. 2000). Theoretical models of objects with envelopes, jets, and accretion disks widely use the concepts of magneto hydrodynamics (see the review of Blaes 2003), i.e. they have to be considered as magnetized cosmic objects. Spectrophotometric observations are used to confirm or reject the theoretical models of these complex cosmic objects (Cherepashchuk 2001).

Integral polarization of radiation from point-like cosmic objects (the intrinsic polarization) arises if the structure of these objects is not axially symmetric with respect to the line of sight. Generally, this asymmetry implies the asymmetry of physical conditions in the cosmic objects and their nearest vicinity, not only the asymmetry of their geometric structure. Thus, the spherical envelope with a dipole magnetic field is not an axially symmetric object, and it can produce non-zero integral linear polarization due to different Faraday rotations of the polarization plane of radiation scattered in various volumes of the envelope.

There are a lot of polarimetric observations of various cosmic objects. For example, Lamy & Hutsemekers (2000) present the optical polarization of 47 quasi-stellar objects. Most QSOs in this catalogue have rather small intrinsic polarization – only 10 objects have $p > 1\%$. The maximum polarization $\cong 6\%$ has

the object B1333+2840. Schmidt & Hines (1999) give the polarization of broad absorption lines for 53 QSOs, where only 15 objects show large ($p > 3\%$) polarization. The catalogue of optical polarization of 83 QSOs (Wills et al. 1992) shows that the fraction of highly polarized ($p > 3\%$) objects is smaller for more distant ($z > 1$) QSOs. The possible explanation of this is given in Gnedin & Silant'ev (2002). The polarimetry of a number of active galaxies is presented in Young et al. (1996). There are many polarimeric observations of supernova explosions (see Leonard et al. 2000). The observed magnitude of the polarization varies from 0.2% up to 2% and is explained as being due to Thomson scattering in aspherical envelopes. We also note the X-ray polarimetric observations of ScoX-1 (Long et al. 1979) and CygX-1 (Long et al. 1980). For ScoX-1 they find $p(2.6 \text{ keV}) \cong 0.4\%$ and $p(5.2 \text{ keV}) \cong 1.31\%$. The CygX-1 gives larger polarization – $p(2.6 \text{ keV}) \cong 2.4\%$ and $p(5.2 \text{ keV}) \cong 5.3\%$. Now the gamma-ray polarimetry is arising. It should be stressed that optical polarimetry can measure very small polarization $\sim 0.01\%$ (see catalogues mentioned above). We do not mention here the numerous polarimetric observations of the usual stars. Some of them can be magnetized and possess magnetized eruptive envelopes (see Chesneau et al. 2003).

This paper deals with the integral polarization that arises due to the existence of Faraday rotation of the polarization plane of the radiation, scattered in various magnetized envelopes. The partly polarized scattered radiation undergoes different Faraday rotations for various scattering volumes in an envelope. As a result, the integral scattered radiation from the envelope acquires non-zero net polarization even if

the envelope is axially symmetric geometrically with respect to the line of sight. The angle of Faraday rotation $\psi \propto \lambda^2$ depends on the wavelength of the radiation. This gives rise to the peak-like form of the polarization degree spectrum $p(\lambda)$ (see Gnedin & Silant'ev 1980, 1984, 1997 and Gnedin et al. 2005). The particular form of the λ-dependence is different for various models of the electron number density, which gives the opportunity to estimate both the magnetic field value and the electron density distribution. This new technique is available if the spectra of polarization are observed; yet in the papers mentioned above, only the regular magnetic field is considered.

It should be noted that the known Zeeman effect technique for estimating the magnetic field in a vicinity of the objects with envelopes is frequently invalid due to the absence of suitable spectral lines. Thus, the Faraday rotation mechanism for polarizing of the integral radiation is a very important additional technique for estimating the existing magnetic fields.

The goal of this paper is to investigate how the spectrum $p(\lambda)$ and the positional angle spectrum $\chi(\lambda)$ in turbulent envelopes change when the magnetic field acquires the fluctuating component. First, we review the mechanism of polarization in non-turbulent magnetized envelopes. Then, we proceed by considering turbulent envelopes in Sect. 3. In Sects. 4 and 5 the spherical and cone-like envelopes are considered. Section 6 deals with the asymptotical behavior of polarization at large wavelengths.

2. Polarization of radiation scattered in non-turbulent envelopes

To start, we write the usual transfer equations for Stokes parameters $I(r, n)$, $Q(r, n)$, and $U(r, n)$ that describe the intensity and linear polarization of radiation:

$$
\begin{aligned}
(n\nabla)I(r, n) &= -\alpha\, I(r, n) + N_e \sigma_T B_I(r, n), \\
(n\nabla)Q(r, n) &= -\alpha\, Q(r, n) - N_e(r)\sigma_T \delta \cos\Theta\, U(r, n) \\
&\quad + N_e \sigma_T B_Q(r, n), \\
(n\nabla)U(r, n) &= -\alpha\, U(r, n) + N_e(r)\sigma_T \delta \cos\Theta\, Q(r, n) \\
&\quad + N_e \sigma_T B_U(r, n),
\end{aligned} \tag{1}
$$

where $\sigma_T = 8\pi r_e^2/3$ is the Thomson cross-section, $r_e = e^2/m_e c^2$ is the classic radius of electron, $\alpha = N_e \sigma_T + k_a$ the extinction factor, k_a true absorption coefficient, $N_e(r)$ the electron number density, n the direction of the light propagation, Θ the angle between n and magnetic field B. The $B_{I,Q,U}$-terms describe the scattering of radiation on free electrons (see for example, Chandrasekhar 1950). Dimensionless parameter δ characterizes the Faraday rotation effect:

$$
\delta = \frac{3}{8\pi^2} \cdot \frac{c\,\omega_B}{r_e \nu^2} \equiv \frac{3\lambda}{4\pi r_e} \cdot \frac{\omega_B}{\omega} \cong 0.8\lambda^2(\mu m)B(G) \tag{2}
$$

where λ and ν are the wavelength and frequency of the scattered light, respectively, and $\omega_B = eB/m_e c$ is the cyclotron frequency.

The angle of Faraday rotation of the polarization plane is:

$$
\psi(n) = \frac{1}{2}\delta\,\tau_T \cos\Theta, \tag{3}
$$

where $\tau_T = N_e \sigma_T s$ is the Thomson optical depth along a path s.

For an optically thin envelope, the Stokes parameters of the single-scattered radiation are determined by the expressions (Gnedin & Silant'ev 1984, 1997; Gnedin et al. 2005):

$$
\begin{aligned}
F_I(n) &= \frac{L}{4\pi R^2} \cdot \frac{3\sigma_T}{16\pi} \int dV \frac{N_e(r)}{r^2} \left\{ \frac{8r^2}{3R_s^2}\left(1 - \sqrt{1 - \frac{R_s^2}{r^2}}\right) \right. \\
&\quad \left. + \left(-\frac{1}{3} + \cos^2\vartheta\right)\sqrt{1 - \frac{R_s^2}{r^2}} \right\},
\end{aligned}
$$

$$
\begin{aligned}
F_Q(n) &= -\frac{L}{4\pi R^2} \\
&\quad \times \frac{3\sigma_T}{16\pi} \int dV \frac{N_e(r)}{r^2}\sqrt{1 - \frac{R_s^2}{r^2}}\sin^2\vartheta\cos 2(\varphi + \psi),
\end{aligned}
$$

$$
\begin{aligned}
F_U(n) &= -\frac{L}{4\pi R^2} \\
&\quad \times \frac{3\sigma_T}{16\pi} \int dV \frac{N_e(r)}{r^2}\sqrt{1 - \frac{R_s^2}{r^2}}\sin^2\vartheta\sin 2(\varphi + \psi), \tag{4}
\end{aligned}
$$

where L is the stellar spectral luminosity (erg s^{-1} Hz^{-1}), ϑ and φ are the polar and azimuthal angles of a radius-vector r in the reference frame with z-axis directed to the observer (along the line of sight n), and R is the distance to the observer. The integration is carried out over all visible volumes of an envelope. We choose the X-axis lying in the plane (nh), where h is the direction of magnetic dipole M for a spherical magnetized envelope, or the direction of the axis of the cone-like envelope (see Fig. 1), $\psi \equiv \psi(n, r)$ is the Faraday rotation angle corresponding to the propagation of the light beam scattered in the point r. This angle can be calculated by path integration along the line of sight:

$$
\psi(n, r) = 0.4\sigma_T \lambda^2(\mu m)\int dl N_e(r')n \cdot B. \tag{5}
$$

The vector r' runs along the line of sight n. The coordinates $r' = (r', \vartheta', \varphi')$ are related to $r = (r, \vartheta, \varphi)$: $\varphi = \varphi'$ and $r\sin\vartheta = r'\sin\vartheta'$, which gives the following expression for the path element: $dl = rd\vartheta'\,\sin\vartheta/(\sin\vartheta')^2$.

Near the surface of a star, the volume element dV is illuminated from the semi-sphere of directions, so the star does not look like a point source of radiation with the flux $L/4\pi r^2$. Dolginov et al. (1995) showed how to change the usual formulae to take this effect into account. Our formulae correspond to the case of the intensity of radiation escaping from the star surface element is isotropic ($I(\mu) = $ const.), where μ is the cosine of the angle between outward normal N to the surface and the direction of the escaping. In Dolginov et al. (1995) the analytic formulae are given for the more realistic case $I(\mu) = A + B\mu$ accounting for the gradient of the Planck-function in an atmosphere.

The considered case $I(\mu) = A$ corresponds to homogeneous distribution of thermal sources in an atmosphere. It gives the lower limit for possible degree of polarization. If $r \gg R_s$, formulae (4) transform to the case of a point-like star that corresponds to the upper limit for polarization. It is seen that the scattered radiation is non-polarized near the star surface, which means that the incident radiation falls isotropically from the

Fig. 1. The position of the cone-like envelope and the various angles used in the text. The dotted line presents the direction to an observer.

semi-sphere of directions. Thus, this effect diminishes (sometimes to ~30%) the net polarization compared with a point-like star. This effect was first taken into account in Pogodin (1992). Usually one supposes that illuminating sources (for brevity we call them "stars") are in LTE-state and radiate the non-polarized light.

Formulae (4) for the Stokes parameters F_I, F_Q, and F_U (erg cm^{-2} s^{-1} Hz^{-1}) take only single-scattered radiation into account. In this approximation by calculation of the degree of polarization $p = \sqrt{F_Q^2 + F_U^2}/F_I$ one can take the direct radiative flux from the star as the flux F_I: $F_I = L/4\pi R^2$. Sometimes one supposes that the direct radiation from the star is obscured by some dense matter (for example, the edge of an accretion disk). In this case the observed radiation flux is equal to F_I from Eq. (4) and the integral polarization from the envelope will be much greater than that considered below.

Clearly, that the flux of single-scattered radiation is proportional to the optical depth of an envelope τ_{env} (the exception, see Sect. 5.1), means the parameters $F_Q(\boldsymbol{n})$ and $F_U(\boldsymbol{n})$ can be presented in the form:

$$F_{Q,U}(\boldsymbol{n}) = \frac{L}{4\pi R^2} \tau_{\text{env}} f_{Q,U}(\delta_s \tau_{\text{env}}, \vartheta_h, \vartheta_0), \tag{6}$$

where $\delta_s = 0.8\lambda^2(\mu\text{m})B_s(\text{G})$ is parameter (2) at the star's surface, and B_s is the magnetic field on some point of this surface (particularly, $B_s = M/R_s^3$ for the dipole magnetic field). The angles ϑ_h are the usual polar angles of magnetic dipole $\boldsymbol{M}$ or the axis $\boldsymbol{h}$ of the cone envelope, and the ϑ_0 is the cone opening angle (see Fig. 1).

The positional angle of polarization χ is calculated from the equation

$$\tan(2\chi) = \frac{f_U}{f_Q}. \tag{7}$$

The case of non-magnetized envelopes follows from Eq. (4) if one takes $\psi = 0$. This case was considered in Dolginov & Silant'ev (1974) and Brown & McLean (1977) (note that in the latter paper in the basic formula (23), factor 2 is omitted).

3. Faraday rotation in turbulent envelopes

Recently Silant'ev (2005) developed the radiative transfer theory for turbulent magnetized atmospheres and found that the averaged Stokes parameters obey the usual radiative transfer equation with new effective (renormalized) kinetic coefficients. Note that the observed Stokes parameters I, Q, U, and V coincide with the statistically averaged quantities if many turbulent "cells" exist in the region of the observation. In turbulent atmosphere all quantities – α, N_e, $\boldsymbol{B}$, I, Q, U, V are stochastic functions consisting of the regular (mean) and fluctuating terms. We denote the mean values by subscript zero, and the fluctuating terms – by prime (example, $\alpha = \alpha_0 + \alpha'$ with $\alpha_0 \equiv \langle\alpha\rangle$ and $\langle\alpha'\rangle \equiv 0, N_e = N_0 + N'_e$). Further, we shall only deal with the averaged Stokes parameters I_0, Q_0 and U_0.

First, the existence of fluctuations manifests itself by the decrease in the extinction factor:

$$\alpha_{\text{eff}} = \alpha_0 \left(1 - \frac{\langle\alpha'^2\rangle}{\alpha_0^2} \tau_1 f_\alpha\right). \tag{8}$$

Here $\tau_1 = \alpha_0 R_1$ is the mean optical depth of the turbulence correlation length R_1, and f_α is the constant value ($f_\alpha \cong 1$) connected with the correlation function $A_\alpha(R/R_1)$ of α'-fluctuations:

$$\langle\alpha'(s)\alpha'(s')\rangle = \langle\alpha'^2\rangle A_\alpha(R/R_1),$$

$$f_\alpha = \int_0^\infty dx\, A(x), \tag{9}$$

where $R = |s - s'|$ is the difference in coordinates s and s' lying at the line of sight. Very often one uses the exponential correlation function $A(x) = \exp(-x)$, for which $f_\alpha = 1$.

The validity of renormalized radiative transfer equations is $\tau_1 \ll 1$. Note that $\alpha_{\text{eff}} \neq \alpha_0$. For the often used "short-correlated" model of turbulence ($R_1 \to 0$), this effect disappears. In practice, this effect is small and does not change the degree of polarization.

If the envelope plasma is turbulent the Faraday effect gives rise to two new effects. First, the fluctuating Faraday rotations produce a net decrease in the linear polarization of every light beam propagating in such a medium. Statistically we observe the sum of the radiation fluxes with very different angles of the polarization plane. Clearly, the mean polarization of radiation will be smaller than in some of the particular realizations. Remember that, in the medium with regular Faraday rotation, the separate light's beam does not change the initial degree of polarization because intensity I and the Stokes parameters Q and U diminish with the same extinction factor α, as is clearly seen from Eqs. (1) and (10). The known depolarization effect for regular Faraday rotations arises when we observe radiation from various volume elements. Magnetic field fluctuations depolarize the radiation at every separate path of the light. This effect occurs even when the magnetic field is almost stochastic.

The second effect is more subtle, as results from superposition of regular Faraday rotation and fluctuations in the extinction factor. The qualitative explanation (see Silant'ev 2005) is as follows. Let the first realization of the stochastic picture have the optical depth $\tau_+ = \tau_0 + \tau' > \tau_0$. In this case the Faraday rotation of the polarization plane is greater than for a mean path τ_0. But simultaneously the magnitude of polarized light intensity (remember that $Q, U \propto \exp(-(\tau_0 + \tau'))$) is less than for optical depth τ_0. For the second realization with $\tau_- = \tau_0 - \tau' < \tau_0$, the Faraday rotation is smaller than the one corresponding to τ_0, but the magnitude of polarized intensity is greater. As a result, the effective Faraday rotation angle is smaller than the mean value ψ_0. If the mean magnetic field $\boldsymbol{B}_0 \equiv \langle \boldsymbol{B} \rangle = 0$, this explanation does not work because, for every realization, there exists magnetic fluctuations $\boldsymbol{B}'$ and $-\boldsymbol{B}'$ with equal probability, and the net Faraday rotation does not arise.

These two effects can be qualitatively derived from the model of two realizations with the parameters $\tau_0 + \tau'$, $\psi_0 + \psi'$, and $\tau_0 - \tau'$, $\psi_0 - \psi'$; for simplicity we consider here that magnetic field $\boldsymbol{B}$ is regular and the fluctuations τ' and ψ' are only due to fluctuations of electron number density N_e'. Indeed, the exact solutions of radiative transfer equations (1) without the source terms are:

$$I_\pm(s) = I(0)\mathrm{e}^{-(\tau_0 \pm \tau')},$$

$$Q_\pm(s) = Q(0)\mathrm{e}^{-(\tau_0 \pm \tau')} \cos 2(\chi_0 \pm \chi'),$$

$$U_\pm(s) = Q(0)\mathrm{e}^{-(\tau_0 \pm \tau')} \sin 2(\chi_0 \pm \chi'), \tag{10}$$

where $I(0)$, $Q(0)$, and $U(0) = 0$ are the initial Stokes parameters at $s = 0$, and s is the path of radiation in the turbulent magnetized atmosphere. Optical depths and positional angles are the path integrals:

$$\tau_0 \pm \tau' = \int_0^s \mathrm{d}s \alpha_0(s) \pm \int_0^s \mathrm{d}s \alpha'(s),$$

$$\chi_0 \pm \chi' = \frac{1}{2}\sigma_\mathrm{T} \int_0^s \mathrm{d}s\, N_0(s)\delta_0(s) \cos\Theta_0(s)$$
$$\pm \frac{1}{2}\sigma_\mathrm{T} \int_0^s \mathrm{d}s N_e'(s)\delta_0(s) \cos\Theta_0(s). \tag{11}$$

Calculation of mean values $I_0(s) = (I_+ + I_-)/2$ etc. for small τ' and χ' gives rise to the formulae:

$$I_0(s) = I(0)\mathrm{e}^{-\tau_0} \cosh(\tau') \cong I(0)\mathrm{e}^{-(\tau_0 - \tau'^2/2)}$$
$$\equiv I(0)\mathrm{e}^{-\tau_\mathrm{eff}} < I(0)\mathrm{e}^{-\tau_0},$$

$$Q_0(s) \cong Q(0)\mathrm{e}^{-\tau_0}\left[\left(1 + \frac{\tau'^2}{2} - 2\chi'^2\right)\cos(2\chi_0)\right.$$
$$\left. + 2\tau'\chi' \sin(2\chi_0)\right],$$

$$U_0(s) \cong Q(0)\mathrm{e}^{-\tau_0}\left[\left(1 + \frac{\tau'^2}{2} - 2\chi'^2\right)\sin(2\chi_0)\right.$$
$$\left. - 2\tau'\chi' \cos(2\chi_0)\right]. \tag{12}$$

Note that these formulae are valid in the general case where the magnetic field is stochastic with the isotropic distribution of

fluctuations. It is seen from Eqs. (12) that the effective optical depth for the intensity

$$\tau_\mathrm{eff} = \tau_0 - \frac{1}{2}\tau'^2 \tag{13}$$

is smaller than the mean optical depth τ_0. The expressions for $Q_0(s)$ and $U_0(s)$ show that effective extinction of the polarization magnitude is greater than for the intensity:

$$P_0(s) \equiv \sqrt{Q_0^2(s) + U_0^2(s)} = P(0)\mathrm{e}^{-(\tau_\mathrm{eff} + 2\chi'^2)}. \tag{14}$$

The additional term $2\chi'^2$ describes the depolarization effect of stochastic Faraday rotations by the propagation of the polarized radiation in a turbulent magnetized medium. This is the statistical effect. The exact expressions (10) demonstrate that $P_\pm(s) = P(0)\exp(-(\tau_0 \pm \tau'))$, i.e. extinction of polarization magnitude is the same as for intensity I, and the degree of polarization does not change ($p_\pm = P_\pm/I_\pm \equiv P(0)/I(0) = p(0)$). Calculation of $U_0(s)/Q_0(s) \equiv \tan(2\chi_\mathrm{eff})$ gives rise to the expression:

$$\chi_\mathrm{eff} = \chi_0 - \tau'\chi', \tag{15}$$

which explains the second effect. Note that $\tau' \propto \alpha'$ and $\chi' \propto N_e'$. The term with $\boldsymbol{B}'$ in χ' disappears because statistically the fluctuations $\boldsymbol{B}'$ and $-\boldsymbol{B}'$ occur with equal probability.

Assuming the Gaussian ensemble of realizations all fluctuating values, Silant'ev (2005) derived the new renormalized transfer equations for average Stokes parameters I_0, Q_0, and U_0:

$$(\boldsymbol{n}\nabla)I_0(\boldsymbol{r}, \boldsymbol{n}) = -\alpha_\mathrm{eff}\, I_0(\boldsymbol{r}, \boldsymbol{n}) + \langle N_e \sigma_\mathrm{T} B_i(\boldsymbol{r}, \boldsymbol{n}) \rangle,$$

$$(\boldsymbol{n}\nabla)Q_0(\boldsymbol{r}, \boldsymbol{n}) = -\alpha_\mathrm{pol}\, Q_0(\boldsymbol{r}, \boldsymbol{n})$$
$$- N_0(\boldsymbol{r})\sigma_\mathrm{T}\delta_\mathrm{eff} \cos\Theta_0\, U_0(\boldsymbol{r}, \boldsymbol{n}) + \langle N_e\sigma_\mathrm{T} B_Q(\boldsymbol{r}, \boldsymbol{n}) \rangle,$$

$$(\boldsymbol{n}\nabla)U_0(\boldsymbol{r}, \boldsymbol{n}) = -\alpha_\mathrm{pol}\, U_0(\boldsymbol{r}, \boldsymbol{n})$$
$$+ N_0(\boldsymbol{r})\sigma_\mathrm{T}\delta_\mathrm{eff} \cos\Theta_0\, Q_0(\boldsymbol{r}, \boldsymbol{n}) + \langle N_e\sigma_\mathrm{T} B_U(\boldsymbol{r}, \boldsymbol{n}) \rangle. \tag{16}$$

Here $N_0(\boldsymbol{r}) \equiv \langle N_e(\boldsymbol{r}) \rangle$ is the average value of the electron number density. The average source functions are presented in Silant'ev (2005). The effective coefficients α_pol and δ_eff have the following form:

$$\alpha_\mathrm{pol} = \alpha_\mathrm{eff} + N_0\sigma_\mathrm{T}\tau_1^{(\mathrm{T})}$$
$$\times \left[\langle\delta'^2\rangle f_B + \delta_0^2 \cos^2\Theta_0 \frac{\langle N'^2\rangle}{N_0^2} f_N\right], \tag{17}$$

$$\delta_\mathrm{eff} = \delta_0 \left[1 - 2\tau_1 \frac{\langle\alpha' N_e'\rangle}{\alpha_0 N_0} f_{\alpha N}\right]. \tag{18}$$

Here α_eff is given in Eq. (8), $\tau_1^{(\mathrm{T})} = N_0\sigma_\mathrm{T}R_1$ is the mean Thomson optical depth of the turbulent correlation length R_1, and $\langle\delta'^2\rangle = (0.8\lambda^2(\mu\mathrm{m}))^2\langle B'^2\rangle/3$ is the rms–value of the fluctuations of the parameter (2). The factors f_B, f_N, and $f_{\alpha N}$ are related to the corresponding correlation functions in Eq. (9). Remember that τ_1 is the total optical depth of the correlation length R_1 including the true absorption. For real envelopes all the effective coefficients depend on the position in an envelope.

The second term in Eq. (17) describes the first effect – the decrease in the polarization degree due to fluctuations of a magnetic field and the electron number density. The term with τ_1 in Eq. (18) characterizes the second effect – decrease in the effective Faraday rotation angle compared with its mean value (remember that $\psi \propto \delta$). The terms with τ_1 in Eq. (8) and $\tau_1^{(T)}$ in Eq. (18) are small, so we neglect them when calculating the polarization from envelopes. The second term in Eq. (17), in contrast, can acquire high values because the parameters δ_0 and δ' can be very large (see Eq. (2)). Considering the single scattering of the radiation in optically thin envelopes, we can neglect the small terms in Eqs. (8), (17), and (18), only the second term in Eq. (17) will be taken into account. As a result, we obtain the following formulae for $F_Q(\boldsymbol{n})$ and $F_U(\boldsymbol{n})$:

$$F_Q(\boldsymbol{n}) = -\frac{L}{4\pi R^2}$$

$$\times \frac{3\sigma_T}{16\pi} \int dV \frac{N_0(r)}{r^2} \sqrt{1 - \frac{R_s^2}{r^2}} \sin^2 \vartheta \cos 2(\varphi + \psi) e^{-C},$$

$$F_U(\boldsymbol{n}) = -\frac{L}{4\pi R^2}$$

$$\times \frac{3\sigma_T}{16\pi} \int dV \frac{N_0(r)}{r^2} \sqrt{1 - \frac{R_s^2}{r^2}} \sin^2 \vartheta \sin 2(\varphi + \psi) e^{-C}, \quad (19)$$

where ψ is the path integral (5). The analogous expression for C is:

$$C(\boldsymbol{n}, \boldsymbol{r}) = \sigma_T (0.8\lambda^2(\mu m))^2 \int dl N_0(r')^2 \tau_1^{(T)}$$

$$\times \left[\frac{\langle B'^2 \rangle}{3} f_B + (\boldsymbol{B}_0 \cdot \boldsymbol{n})^2 \frac{\langle N_e'^2 \rangle}{N_0^2} f_N \right]. \quad (20)$$

Here $\boldsymbol{B}_0(r)$ is the regular component of the magnetic field. Note that the parameter $\langle \delta'^2 \rangle$ does not depend on the angles in isotropic turbulence where $\langle (\boldsymbol{B}' \cdot \boldsymbol{n})^2 \rangle = \langle B'^2 \rangle/3$. The Faraday rotation angle ψ in Eqs. (19) only depends on the regular component of the magnetic field.

4. Spherical envelope with a dipole magnetic field

A spherical envelope with a regular dipole magnetic field $\boldsymbol{B}_0(r)$

$$\boldsymbol{B}_0(r) = \frac{3(\boldsymbol{M} \cdot \boldsymbol{r})\boldsymbol{r} - \boldsymbol{M}r^2}{r^5} \quad (21)$$

was consider in detail in Gnedin et al. (2005). Thus, our aim here is to investigate how the polarization spectrum $p(\lambda)$ and the spectrum of the positional angle $\chi(\lambda)$ change under the influence of magnetic field fluctuations $\boldsymbol{B}'$ and the electron number density fluctuations N_e'. It is convenient to choose the direction of magnetic moment $\boldsymbol{M}$ lying in the plane (XZ), where the Z-axis is directed along the line of sight to the observer $\boldsymbol{n}$.

The Faraday rotation angle (5) has the following analytical form (see Gnedin et al. 2005):

$$\psi(\boldsymbol{n}, \boldsymbol{r}) = \frac{\delta_s \tau_{env}}{30\rho^4} \left\{ \frac{\cos \vartheta_m}{(1 + \cos \vartheta)^2} \left[-4 + 7\cos \vartheta \right. \right.$$

$$\left. \left. + 18 \cos^2 \vartheta + 9 \cos^3 \vartheta \right] + 9 \sin \vartheta_m \cos \varphi \sin \vartheta \right\}. \quad (22)$$

Here $\delta_s = 0.8\lambda^2(\mu m) M/R_s^3$ is the parameter (2) at the magnetic equator of the star surface, R_s is the radius of a star, $\tau_{env} = N_s \sigma_T R_s$ is the radial optical depth of an envelope, $\rho = r/R_s$ is the dimensionless distance of the volume element in Eqs. (19). For the electron number density we have chosen $N_0(r) = N_s/\rho^2$. The angles ϑ and ϑ_m are the usual polar angles between the direction to an observer $\boldsymbol{n}$ and radius-vector $\boldsymbol{r}$ and $\boldsymbol{M}$, respectively, while φ is azimuthal angle of $\boldsymbol{r}$ (see Fig. 1).

To investigate the influence of turbulent fluctuations $\boldsymbol{B}'$ and N_e' on the spectra $p(\lambda)$ and $\chi(\lambda)$, we assume that the level of these fluctuations is constant compared with its mean values. Besides, we assume that the optical depth of turbulent cells $\tau_1^{(T)}$ is also constant in the envelope. These are rather natural assumptions and they simplify formulae for $C(\boldsymbol{n}, \boldsymbol{r})$. As a result, we obtain:

$$C(\boldsymbol{n}, \boldsymbol{r}) = C_B(\boldsymbol{n}, \boldsymbol{r}) + C_N(\boldsymbol{n}, \boldsymbol{r}), \quad (23)$$

where C_B and C_N corresponds to the first and second terms in Eq. (20). The expression C_B acquires the form:

$$C_B(\boldsymbol{n}, \boldsymbol{r}) = \gamma_B f_B \frac{\tau_1^{(T)}}{\tau_{env}} \cdot \frac{(\delta_s \tau_{env})^2}{(\rho \sin \vartheta)^7} \int_0^\vartheta d\vartheta' \sin^6 \vartheta', \quad (24)$$

$$C_N(\boldsymbol{n}, \boldsymbol{r}) = \gamma_N f_N \frac{\tau_1^{(T)}}{\tau_{env}} \cdot \frac{(\delta_s \tau_{env})^2}{(\rho \sin \vartheta)^7}$$

$$\times \int_0^\vartheta d\vartheta' \sin^6 \vartheta' \left[\cos \vartheta_m \left(3\cos^2 \vartheta' - 1 \right) \right.$$

$$\left. + 3 \sin \vartheta_m \cos \varphi \sin \vartheta' \cos \vartheta' \right]^2. \quad (25)$$

Here we use the notations:

$$\gamma_B = \frac{\langle B_s'^2 \rangle}{B_s^2}, \qquad \gamma_N = \frac{\langle N_e'^2 \rangle}{N_s^2}, \quad (26)$$

where $B_s = M/R_s^3$ is the characteristic mean magnetic field at the star surface, $\langle B_s'^2 \rangle$ is the level of magnetic fluctuations at star's surface ($\langle B'^2(\rho) \rangle = \langle B_s'^2 \rangle/\rho^6$), $\langle N_e'^2(\rho) \rangle = \langle N_e'^2 \rangle/\rho^2$, and N_s is the mean electron number density at the star surface. The values $\langle B_s'^2 \rangle$ and $\langle N_e'^2 \rangle$ are the rms values of fluctuations at the star surface, i.e. the parameters γ_B and γ_N are independent of ρ. The integrals in Eqs. (24) and (25) are standard and can be taken, for example, from Gradshteyn & Ryzhik (1994).

In Fig. 2 we present the results of the numerical calculations of $p(\lambda)/\tau_{env}$ and $\chi(\lambda)$ for the case of purely magnetic fluctuations ($C_N = 0$) for various values of parameter $b = \gamma f_B(\tau_1^{(T)}/\tau_{env})$. Remember that parameter $\sqrt{\delta_s \tau_{env}} \propto \lambda$; i.e. our figures are the spectra of the polarization degree and the positional angle. In Fig. 3 the same is presented for the case of electron number density fluctuations ($C_B = 0$). The positive values of positional angle χ correspond to the left-hand rotation from the plane ($\boldsymbol{Mn}$) if we see along direction $\boldsymbol{n}$ to an observer. For $\vartheta_m = 90°$ the plane of electric field oscillations coincides with ($\boldsymbol{Mn}$)-plane ($\chi = 0$).

First of all we see that the magnetic fluctuations change the spectra $p(\lambda)$ and $\chi(\lambda)$ very strongly when compared with the case of the electron number density fluctuations. What is the reason for this difference? The difference between $C_B(\boldsymbol{n}, \boldsymbol{r})$
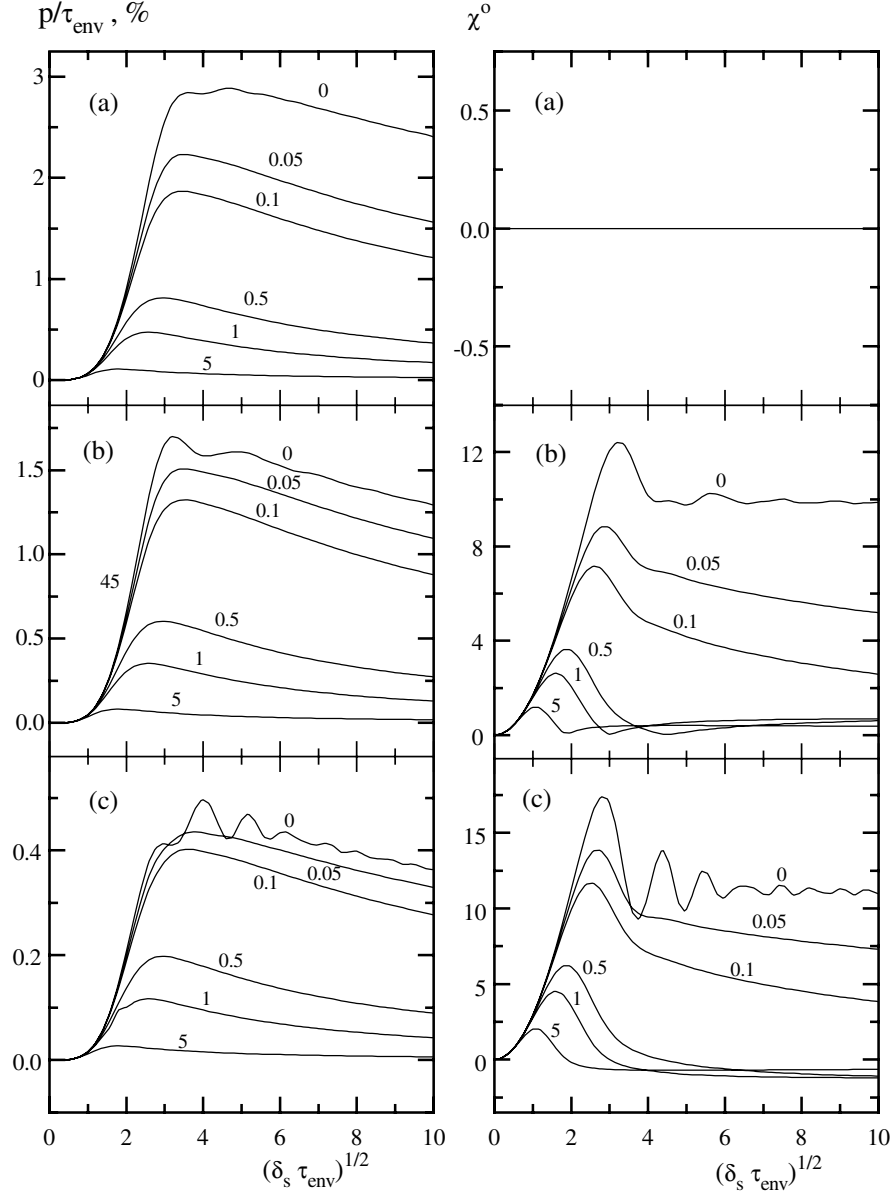
Fig. 2. The degree of polarization and the positional angle of radiation scattered in a spherical envelope with a magnetic dipole field. The cases **a)**, **b)**, and **c)** correspond to the inclination angles of the magnetic dipole M: $\vartheta_m = 90°$, $60°$, and $30°$. The numbers near curves denote the values of the parameter $b = \langle B_s'^2 \rangle / B_s^2 f_B(\tau_1^{(T)}/\tau_{\text{env}})$.

and $C_N(\boldsymbol{n}, \boldsymbol{r})$ consists of the additional term $\cos^2\Theta_0$ in expression (25) (the term in square brackets) for C_N compared with Eq. (24) for C_B. Remember that Θ_0 is the angle between regular magnetic field $\boldsymbol{B}_0$ and the line of sight $\boldsymbol{n}$. The volumes of an envelope with small $\cos\Theta_0$ contribute the most to the integral polarization from the envelope, the factor C_N is smaller than the C_B -coefficient. This explains the relatively small contribution of the electron number density fluctuations compared to the contribution from the magnetic field fluctuations. For this reason one can only take the action of magnetic fluctuations into account.

In contrast to the scalar electron number density, the vector magnetic field can have mean value a zero. In this case the γ_B – parameter in Eq. (24) has to be taken equal to unity, and the parameter δ_s^2 is equal to the value $\delta_s^2 = (0.8\,\lambda^2(\mu m))^2 \langle B_s'^2 \rangle$. Here

$\langle B_s'^2 \rangle$ is the rms-value of magnetic fluctuations at the surface of a star. If the $\langle B_s'^2 \rangle \gg B_s^2$, then the b-parameter can be very large. The behavior of the positional angle χ in both cases is qualitatively the same. Note that $\chi \to 0$ for $\sqrt{\delta_s \tau_{\text{env}}} \to \infty$. For an envelope without any fluctuations $\chi \to 11.25°$ (see Sect. 6).

The spherical envelope without the regular magnetic field can give the integral polarization if the distribution of magnetic fluctuations $\langle B'^2(\boldsymbol{r}) \rangle$ is not axially symmetric along the line of sight $\boldsymbol{n}$.

5. Polarization from magnetized turbulent cone-like jets

Cone-like jets possess integral polarization (see, Dolginov & Silant'ev 1974 and Dolginov et al. 1995) even without any
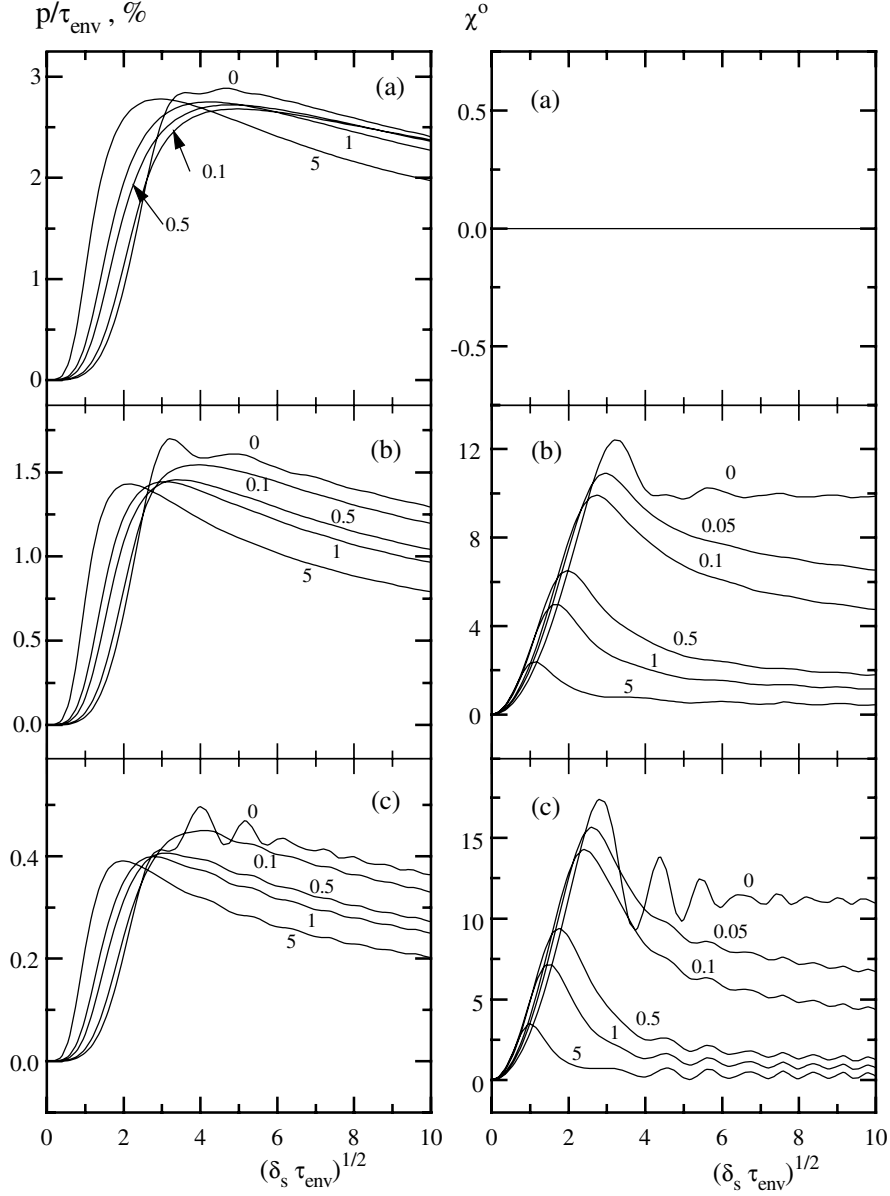
Fig. 3. Same as in Fig. 2 for the turbulent electron number density fluctuations. Parameter $b = \langle N_e'^2 \rangle / N_s^2 f_N (\tau_1^{(T)} / \tau_{\text{env}})$.

magnetic field, due to the absence of the axial symmetry of the scattering picture:

$$p = \frac{|F_Q|}{L/4\pi R^2} = \frac{3}{16} \cdot \frac{\pi}{4} \tau_{\text{env}} \cos \vartheta_0 \sin^2 \vartheta_0 \sin^2 \vartheta_h, \tag{27}$$

where ϑ_h is the polar angle of the cone-axis $\boldsymbol{h}$, and ϑ_0 the cone opening angle (see Fig. 1). The factor $\pi/4$ arises when we take into account that the star is not a point-like source of radiation (for the case $N_e \propto r^{-2}$ and $I(\mu) = \text{const.}$). Thus, Eq. (27) gives the lower limit for the polarization degree. The electric field oscillations of scattered radiation are perpendicular to the plane $(\boldsymbol{nh})$ that corresponds to $\chi = 0$ in Fig. 4. The value τ_{env} is the radial Thomson optical depth of the cone-like envelope. For the model with $N_0(r) = N_s(R_s^2/r^2)$, it is equal to $N_s \sigma_T R_s$.

The integration in formulae (19) can be easily performed using the coordinate system $(\boldsymbol{h})$ with Z-axis along the symmetry axis of a cone and with X-axis lying in the plane $(\boldsymbol{nh})$. The

radius-vector $\boldsymbol{r}$ of the volume element dV in this system is characterized by (r, ϑ, φ), and in the system $(\boldsymbol{n})$ with Z-axis along $\boldsymbol{n}$ by (r, θ, ϕ). According to formulae of spherical geometry, one has the relations:

$$\cos \theta = \cos \vartheta \cos \vartheta_h - \sin \vartheta \sin \vartheta_h \cos \varphi,$$

$$\cos \vartheta = \cos \theta \cos \vartheta_h + \sin \theta \sin \vartheta_h \cos \phi,$$

$$\sin \theta \sin \phi = \sin \vartheta \sin \varphi. \tag{28}$$

The Faraday rotation angle $\psi(\boldsymbol{n}, \boldsymbol{r})$ (see Eq. (5)) can be presented analytically for the following forms of the electron number density and the mean magnetic field:

$$N_0(r) = \frac{N_s}{\rho^n}, \qquad \boldsymbol{B}_0(r) = \frac{B_s}{\rho^m} \boldsymbol{e}_r, \tag{29}$$
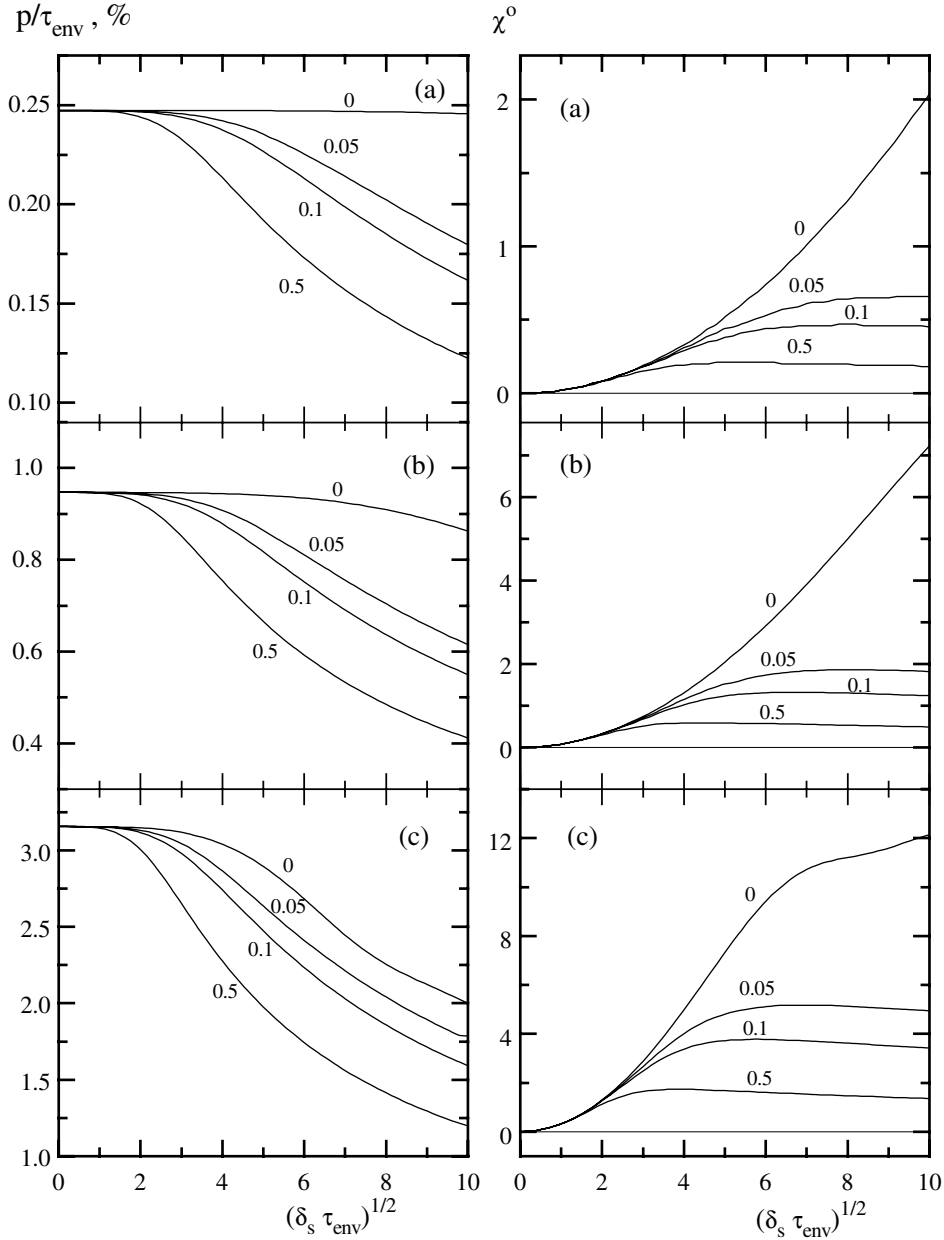
Fig. 4. The degree of polarization and the positional angle of the radiation scattered in a cone-like envelope with $\vartheta_h = 90°$. The cases **a)**, **b)**, and **c)** correspond to $\vartheta_0 = 7.5°$, $15°$ and $30°$. The numbers near curves denote the values of parameter $b = \langle B_s'^2 \rangle / B_s^2 f_B (\tau_1^{(T)} / \tau_{env})$.

where $e_r = r/r$ is the radial unit vector, and $\rho = r/R_s$ is the dimensionless distance from the center of a star. We obtain the following expression:

$$\psi(n, r) = \frac{\delta_s \tau_{env}(n-1)}{2(n+m-1)\rho^{n+m-1}} \left[1 - \left(\frac{\sin \theta_b}{\sin \theta} \right)^{n+m-1} \right]. \tag{30}$$

Here $\delta_s = 0.8\lambda^2(\mu m)B_s$ is parameter (2) at the surface of a star, and the angle θ_b corresponds to the point where the line of sight transverse the boundary of the envelope. The expression for τ_{env} acquires the form:

$$\tau_{env} = \frac{N_s \sigma_T R_s}{n-1}. \tag{31}$$

This expression is valid for $n \geq 2$. Our numerical calculation will be made for $n = 2$ and $m = 2$. General expressions (30)

and (31) are then used to obtain the asymptotic behavior of $p(\lambda)$ for large λ.

Using the formulae (28) we find the expression:

$$\cos \theta_b = \frac{g + \sqrt{g^2 - ac}}{a}, \tag{32}$$

where the values a, c, and g are:

$$a = \sin^2 \theta - \sin^2 \vartheta \sin^2 \vartheta_h \sin^2 \varphi,$$

$$c = \sin^2 \theta (\cos^2 \vartheta_h \cos^2 \vartheta_0 - \sin^2 \vartheta_h \sin^2 \vartheta_0)$$

$$+ \sin^2 \vartheta_h \sin^2 \vartheta \sin^2 \varphi,$$

$$g = \sin^2 \theta \cos \vartheta_h \cos \vartheta_0. \tag{33}$$

If the cone-like jet is perpendicular to the line of sight ($\vartheta_h = 90°$), the polarization of radiation acquires the maximum. For this case one has the relation $\sin\theta_b \cos\vartheta = \sin\theta \cos\vartheta_0$, and the ψ-expression is simpler:

$$\psi(\boldsymbol{n}, \boldsymbol{r}) = \frac{\delta_s \tau_{env}(n-1)}{2(n+m-1)\rho^{n+m-1}}\left[1 - \left(\frac{\cos\vartheta_0}{\cos\vartheta}\right)^{n+m-1}\right]. \quad (34)$$

Note that if the angle $\vartheta_0 \geq \vartheta_h$ and $\vartheta_h \leq 90°$, then the equality $\theta_b = 0$ takes place.

We have found in the previous section that the electron number density fluctuations give a rather small decrease of the integral polarization compared to the magnetic field fluctuations. For this reason we only consider the latter here. The general expression for C_B has the form:

$$C_B(\boldsymbol{n}, \boldsymbol{r}) = b\frac{(n-1)(\delta_s\tau_{env})^2}{3(\rho\sin\theta)^{n+2m-1}}\int_{\theta_b}^{\theta}d\theta'(\sin\theta')^{n+2m-2}, \quad (35)$$

where $b = (\gamma_B f_B)(\tau_1^{(T)}/\tau_{env})$ with γ_B given in Eq. (26). If the regular magnetic field is absent, we assume that $\langle B'^2\rangle = \langle B_s'^2\rangle/\rho^{2m}$ and $\delta_s^2 = (0.8\lambda^2)^2\langle B_s'^2\rangle$. In this case $b = f_B\,\tau_1^{(T)}/\tau_{env}$.

The results of calculations for the model (29) with $n = 2$ and $m = 2$ are presented in Fig. 4. We see that the spectra of polarization (remember that $\sqrt{\delta_s\tau_{env}} \propto \lambda$) strongly change its forms compared with ones without the turbulent fluctuations ($b = 0$). Note that these spectra are practically independent of regular magnetic field for all the parameters b mentioned above. This means that the mechanism of stochastic Faraday depolarization for $\sqrt{\delta_s\tau_{env}} \geq 1-2$ is more effective than the usual depolarization due to various rotation angles from different volumes of the envelope. The positive positional angles χ correspond to right-hand rotation from the axis Y (see Fig. 1) if we see along the direction $\boldsymbol{n}$ to an observer. The cone jet without the regular magnetic field has $\chi = 0$ because the magnetic fluctuations are assumed to be isotropic. Thus, non-zero values of χ are due to the existence of a regular magnetic field. The spectra $\chi(\lambda)$ are more sensitive to the existence of a regular magnetic field than the $p(\lambda)$-spectra. Note that $\chi(\lambda) \to 0$ for the turbulent envelope at $\sqrt{\delta_s\tau_{env}} \to \infty$, and it tends to 15° for the envelope with a pure regular magnetic field (see next section).

If we have two equal cone-like jets with the opposite axis, then for $\vartheta_h = 90°$ the total polarization will be twice larger with the same positional angle. For $\vartheta_h \neq 90°$ the situation is more complex. For many cases with $\vartheta_h \geq \vartheta_0$ one can roughly take the degree of polarization also is twice larger than for one jet and the net positional angle to be near zero because the oppositely inclined jets have opposite signs of χ.

5.1. Optically thick narrow jet-like envelopes

The maximum polarization $p_{max}(\vartheta_h, \vartheta_0, \tau_{env})$ from the cone-like envelope corresponds to the absence of any magnetic field (see Eq. (27)). The upper limit for p_{max} takes place for a point-like star at $\vartheta_h = 90°$ and $\vartheta_0 \cong 55°$ ($\cos\vartheta_0 = 1/\sqrt{3}$): $p_{max} \cong 7.2\tau_{env}\%$. Remember that τ_{env} in Eq. (27) is the radial Thomson optical depth of the cone-like envelope, and it was assumed $\tau_{env} \ll 1$. Thus, for $\tau_{env} = 0.2$ the upper limit polarization is equal to $\approx 1.4\%$. For angles $\vartheta_0 = 30°, 15°$, and $7.5°$,

the polarization degree is smaller: 0.8%, 0.24%, and 0.06%, respectively. These are rather low values of polarization (but quite observable by modern polarimeters).

In reality the cone-like envelopes with small ϑ_0 ($\vartheta_0 \leq 30°$) can produce greater polarization. For these envelopes the second scattering of radiation can be negligible even at $\tau_{env} \approx 0.5-2$ (depending on the cone opening angle ϑ_0). Simultaneously, such envelopes have small optical depth in the direction perpendicular to the axis $\boldsymbol{h}$, so for our case $N_e \propto 1/r^2$ and $\vartheta_h = 90°$, the maximum value for this optical depth is equal to $\tau_{\perp max}(\rho) = \tau_{env}\vartheta_0/\rho$ ($\rho = r/R_s$ is dimensionless distance from the center of a star). The value $\tau_{\perp max}(\rho)$ corresponds to the perpendicular distance lying in the plane ($\boldsymbol{nh}$) from the axis $\boldsymbol{h}$ of an envelope. Note that the radial optical depth $\tau_{env}(\rho) = \tau_{env}(1 - 1/\rho)$. It acquires the value $\tau_{env}/2$ at $\rho = 2$, which is the characteristic distance where most single scatterings occur. For $\vartheta = 30°, 15°$, and $7.5°$ and $\tau_{env} = 1$, the characteristic values $\tau_{\perp max}(2)$ are equal to 0.26, 0.13, and 0.065, respectively.

To estimate the contribution of multiple scattered radiation (for narrow envelopes this means second scattered photons), we have to calculate the values $F_I(\boldsymbol{n})$ and $F_{Q,U}(\boldsymbol{n})$ (see Eqs. (4)) with the additional factors $\exp(-\tau_{env}(\rho))$ and $\exp(-\tau_{\perp}(\rho, \vartheta, \varphi))$. The first factor describes the extinction of star's radiation intensity by virtue of its propagation into a cone-like envelope. The second factor describes the extinction of single-scattered radiation by its escaping from the envelope. Below we consider the point-like star with the envelope perpendicular to the line of sight ($\vartheta_h = 90°$). The explicit formula for $\tau_{\perp}$ is:

$$\tau_{\perp}(\rho, \vartheta, \varphi) = \frac{\tau_{env}}{\rho\cos\vartheta} \cdot \frac{1}{\sqrt{1 + \tan^2\vartheta\sin^2\varphi}}$$

$$\times\left[\arctan\frac{\sqrt{\tan^2\vartheta_0 - \tan^2\vartheta\sin^2\varphi}}{\sqrt{1 + \tan^2\vartheta\sin^2\varphi}}\right.$$

$$\left. + \arctan\frac{\tan\vartheta\cos\varphi}{\sqrt{1 + \tan^2\vartheta\sin^2\varphi}}\right]. \quad (36)$$

Due to the narrowness of the cone-like envelopes, the probability of the second scattering in directions along the axis is rather small, and is proportional to the small solid angle $\pi\vartheta_0^2$. The probability is higher of the second scattering into the vast solid angles perpendicular to the cone axis $\boldsymbol{h}$. Physically $\tau_{\perp}(\rho, \vartheta, \varphi)$ is determined by the second scattering events occuring before escaping the envelope. The comparison of the parameters $F_I(\boldsymbol{n})$ and $F_Q(\boldsymbol{n})$ calculating without the factor $\exp(-\tau_{\perp})$ with those taking into account this factor, demonstrate that for $\tau_{env} = 2$ the relative difference is equal to 15, 31, and 66% for the angles $\vartheta_0 = 7.5, 15$, and 30°, respectively. At $\tau_{env} = 1$ these differences are 6.5, 13.3, and 28%. For $\tau_{env} = 0.5$ they are smaller – 3, 6, and 13%, respectively. Thus, we can neglect the secondly scattered photons for $\tau_{env} \leq 0.5$ for envelopes with $\vartheta_0 \simeq 30°$. For the envelopes with $\vartheta_0 = 15$ and $7.5°$

the corresponding τ_{env} are equal to 1 and 2. This means that we can neglect the factor $\exp(-\tau_\perp)$ for lower values τ_{env} than those mentioned above. Note that the relative differences of the parameters F_I and F_Q are practically the same. Of course, we take the factor $\exp(-\tau_{\text{env}}(\rho))$ into account in all the cases. Due to a wider variety of the scattering angles, the secondly scattered photons contribute less to the integral polarization from the envelopes than do the single-scattered ones.

To take the large $\tau_{\text{env}}(\rho)$ into account in narrow cone-like envelopes, we include in the integrands of Eqs. (4) and (19) the additional term $\exp(-\tau_{\text{env}}(\rho))$ that describes the extinction of incident light inside the envelope by the radial propagation. For the case of non-magnetized envelopes with an illuminating point-like star, this changes Eq. (27) as follows:

$$p = \frac{3}{16}(1 - e^{-\tau_{\text{env}}})\cos\vartheta_0 \sin^2\vartheta_0 \sin^2\vartheta_h. \tag{37}$$

This expression is valid for all models of the electron number density $N_e(r)$. For $\tau_{\text{env}} \ll 1$, formula (37) coincides with Eq. (27) for a point-like star (without the factor $\pi/4$). The term $\exp(-\tau_\perp)$ was omitted by derivation of formula (37), which means that we restict ourselves to the conditions mentioned above: $\tau_{\text{env}} \leq 0.5$ for $\vartheta_0 \leq 30°$, $\tau_{\text{env}} \leq 1$ for $\vartheta_0 \leq 15°$ and $\tau_{\text{env}} \leq 2$ for $\vartheta_0 \leq 7.5°$. Of course, the angle ϑ_h needs to be near the value $90°$. Comparison of Eqs. (37) and (27) shows that Eq. (27) can be used up to $\tau_{\text{env}} \approx 0.5$.

The substitution of terms $\exp(-\tau(\rho))$ and $\exp(-\tau_\perp(\rho, \vartheta, \varphi))$ into Eqs. (19) gives the polarization for magnetized cone-like narrow envelopes with large radial optical depth. We calculated this polarization for a point-like star. This corresponds to the upper limit for polarization. The results of calculations are presented in Fig. 5, where all the parameters are the same as in Fig. 4. Thus, these figures present the lower and upper limits of polarization.

6. Spectrum of polarization at large wavelengths

The dependence of values $\psi(\boldsymbol{n}, \boldsymbol{r})$ and $C(\boldsymbol{n}, \boldsymbol{r})$ on the wavelength λ is different: $\psi \propto \lambda^2$ and $C \propto \lambda^4$. It means that at large λ (i.e. at large $\delta_s\tau_{\text{env}}$), the decrease in polarization due to chaotic Faraday rotations (see expression (17) for α_{pol}) at every light path is more effective than the decrease in integral polarization due to different regular Faraday rotations from various volume elements. First we obtain the wavelength dependence of $p(\lambda)$ when the turbulence is absent ($C(\boldsymbol{n}, \boldsymbol{r}) = 0$). Clearly, in this case the main contribution to the integral polarization arises from far parts of an envelope where Faraday rotation is not very strong. In these parts the star can be considered as a point-like source of radiation. Our derivation uses the transition to a new dimensionless distance $x = (\delta_s\tau_{\text{env}})^{1/(n+m-1)}/\rho$ (see expression (34) for $\psi(\boldsymbol{n}, \boldsymbol{r})$). The corresponding x-integrals in Eqs. (4) will be from zero up to a high value $(\delta_s\tau_{\text{env}})^{1/(n+m-1)}$ that we replace by ∞. As a result, we obtain the λ-dependence:

$$p(\lambda) \propto \lambda^{-\frac{2(n-1)}{n+m-1}}, \qquad (\delta_s\tau_{\text{env}})^{1/(n+m-1)} \gg 1. \tag{38}$$

For the electron number density $N_0 = N_s/\rho^2$ ($n = 2$) used in our calculations, we have

$$p(\lambda) \propto \frac{1}{\sqrt{\lambda}} \tag{39}$$

for any envelope with a dipole magnetic field ($m = 3$), and

$$p(\lambda) \propto \frac{1}{\lambda^{2/3}} \tag{40}$$

for a cone-like envelope with the radial magnetic field $\boldsymbol{B}_0(\boldsymbol{r}) = \boldsymbol{e}_r B_s/\rho^2$ ($m = 2$). Remember that Eqs. (38)–(40) describe $p(\lambda)$ for those envelopes without turbulence.

For turbulent envelopes, the exponential term $\exp(-C)$ in Eqs. (19) varies more rapidly with the radius than do the terms with $\psi(\boldsymbol{n}, \boldsymbol{r}) \propto (\delta_s\tau_{\text{env}})$, because $C(\boldsymbol{n}, \boldsymbol{r}) \propto (\delta_s\tau_{\text{env}})^2$. In this case we introduce the new distance $x = (\delta_s\tau_{\text{env}})^{2/(n+2m-1)}/\rho$ and take $\psi = 0$ in Eqs. (19). This gives the following λ-dependence:

$$p(\lambda) \propto \lambda^{-\frac{4(n-1)}{n+2m-1}}, \qquad (\delta_s\tau_{\text{env}})^{2/(n+2m-1)} \gg 1. \tag{41}$$

For the electron number density $N_0 = N_s/\rho^2$ used in our calculations we have

$$p(\lambda) \propto \frac{1}{\lambda^{4/7}} \tag{42}$$

for any turbulent envelope with dipole magnetic field ($m = 3$), and

$$p(\lambda) \propto \frac{1}{\lambda^{4/5}} \tag{43}$$

for a cone-like turbulent envelope with the radial magnetic field $\boldsymbol{B}_0(\boldsymbol{r}) = \boldsymbol{e}_r B_s/\rho^2$ ($m = 2$).

Taking $\psi = 0$ in Eqs. (19), we obtain $F_U = 0$ and, as a result, the positional angle $\chi = 0$; i.e. for large λ the effective electric field oscillations are perpendicular to the plane ($\boldsymbol{Mn}$) for the spherical envelope with a magnetic dipole field, and are perpendicular to ($\boldsymbol{hn}$) for cone-like jet.

For the case of non-turbulent envelopes with $N_0 = N_s/\rho^2$, we can demonstrate that $\chi \to \pi/(4(m+1))$ for a large λ. For this case the Faraday rotation angle $\psi(\boldsymbol{n}, \boldsymbol{r})$ acquires the general form:

$$\psi(\boldsymbol{n}, \boldsymbol{r}) = \frac{\delta_s\tau_{\text{env}}}{\rho^{m+1}} \cdot K(\vartheta, \varphi). \tag{44}$$

Function $K(\vartheta, \varphi)$ also depends on other parameters of an envelope, for example, ϑ_m or ϑ_h. Let us introduce the new variable $x = [\delta_s\tau_{\text{env}}K(\vartheta, \varphi)]^{1/(m+1)}/\rho$. The ρ-integration is replaced by x-integration with the limits $(0, (\delta_s\tau_{\text{env}}K(\vartheta, \varphi)^{1/(m+1)})$. If we take ∞ instead of the upper limit, then the Stokes parameters F_Q and F_U in Eqs. (4) will differ only by the different x-integrals:

$$F_Q \propto \int_0^\infty dx \cos(x^{m+1}) = \Gamma\left(1 + \frac{1}{m+1}\right)\cos\frac{\pi}{2(m+1)},$$

$$F_U \propto \int_0^\infty dx \sin(x^{m+1}) = \Gamma\left(1 + \frac{1}{m+1}\right)\sin\frac{\pi}{2(m+1)}. \tag{45}$$

The values of the integrals were taken from Gradshtein & Ryzhik (1994), and $\Gamma(x)$ is the gamma-function. According to Eq. (7) we obtain

$$\chi_{\text{lim}} = \frac{\pi}{4(m+1)}. \tag{46}$$

For a non-turbulent spherical envelope with the dipole magnetic field ($m = 3$), this formula gives $\chi_{\text{lim}} = 11.25°$, and

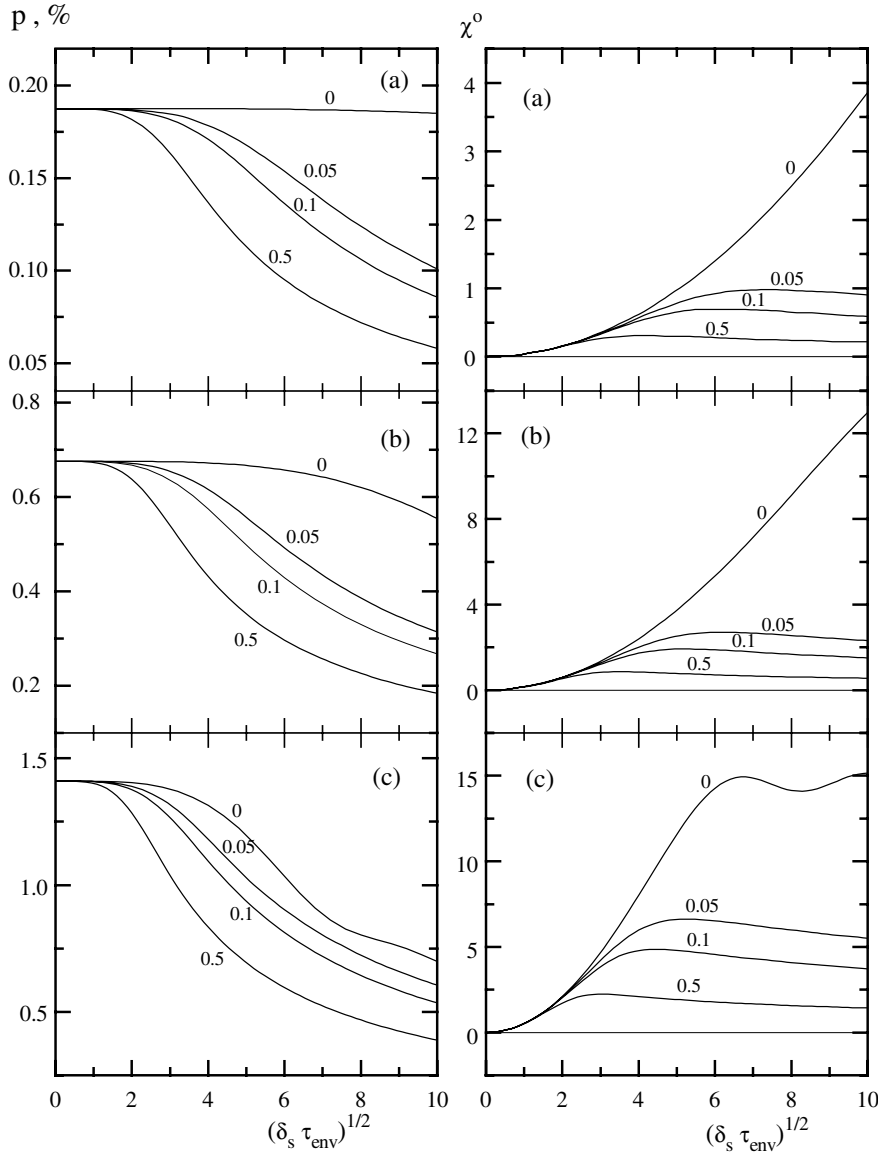**Fig. 5.** The degree of polarization and the positional angle of the radiation scattered in a cone-like narrow envelope with $\vartheta_h = 90°$ and $\tau_{env} = 1, \vartheta_0 = 7.5°$ (case **a**)), $\tau_{env} = 1, \vartheta_0 = 15°$ (case **b**)), and $\tau_{env} = 0.5, \vartheta_0 = 30°$ (case **c**)). The numbers near curves denote the values of the parameter $b = \langle B_s'^2 \rangle / B_s^2 f_B(\tau_1^{(T)}/\tau_{env})$.

for cone-like jet with radial magnetic field ($m = 2$) one has $\chi_{lim} = 15°$. Note that this asymptotic behavior does not depend on the geometry of the envelope, but is affected instead by the radial dependencies of the electron density and the magnetic field.

Thus, by analyzing the observed functions $p(\lambda)$ and $\chi(\lambda)$ for large λ, we can determine if turbulence exists in an envelope. Then one can reconstruct the ρ-dependence of N_0 and $\boldsymbol{B}_0$ and estimate the level of magnetic fluctuation b.

For cone-like jets the asymptotic behavior (43) takes place for $\sqrt{\delta_s \tau_{env}} \geq 10-20$, whereas the asymptotic law (40) for the regular magnetic field occurs for higher values of this parameter $\sqrt{\delta_s \tau_{env}} \geq 100$. For this reason the difference between these two cases can be established even in the range $\sqrt{\delta_s \tau_{env}} \approx 5-10$. The narrow cone-like jets with $\tau_{env} \leq 0.5-2$ (see Sect. 5.1) have the same asymptotical behavior.

7. Conclusion

In this paper we investigate the influence of the fluctuations of a magnetic field $\boldsymbol{B}'$ and the electron number density N_e' on the polarization degree spectra $p(\lambda)$ and the positional angle spectra $\chi(\lambda)$ of the radiation that is single-scattered in a magnetized turbulent circumstellar envelope. The envelopes are assumed to be optically thin and the observed integral polarization of the scattered radiation is calculated. Two models of the envelopes were considered: a spherical envelope with the magnetic dipole field and the cone-like jet with the radial magnetic field. We take into account that the central source ("star") is not a point-like source of non-polarized radiation and have excluded the contribution of the invisible part of an envelope. The assumed star surface intensity $I(\mu) = $ const. corresponds to a lower limit for possible polarization. In contrast, the model of a point-like source gives the upper limit for polarization. It is shown that

in narrow cone-like ($\vartheta_0 \leq 30°$) envelopes the second scattering of radiation is negligible up to a radial optical thickness of $\tau_{env} \cong 0.5-2$ (depending of the cone opening angle ϑ_0). In this case the single - scattered radiation produces maximum polarization $p \simeq 1.4\%$ at $\tau_{env} = 0.5$ (see Fig. 5).

The magnetic field $\boldsymbol{B}(\boldsymbol{r}) = \boldsymbol{B}_0(\boldsymbol{r}) + \boldsymbol{B}'(\boldsymbol{r})$ and the concentration of the plasma electrons $N_e(\boldsymbol{r}) = N_0(\boldsymbol{r}) + N'_e(\boldsymbol{r})$ are considered as a sum of the mean values and fluctuating components (denoted by primes). To investigate the problem we have used the recently published theory of radiative transfer in turbulent magnetized atmospheres (Silant'ev 2005). According to this theory the chaotic Faraday rotations due to the fluctuations $\boldsymbol{B}'$ and N'_e in a magnetized atmosphere give rise to the additional decrease in the degree of linear polarization $p(\lambda)$ of the propagating radiation.

The numerical calculations demonstrate that the influence of the electron concentration fluctuations is less than the contribution of magnetic fluctuations. The additional extinction coefficient for Stokes parameters Q and U is proportional to λ^4, whereas the Faraday rotation angle in a regular magnetic field $\propto \lambda^2$. For this reason for large λ, the extinction of polarized components on every light path is more effective than the integral depolarization due to different Faraday rotations from various volume elements of an envelope. This changes the spectra $p(\lambda)$ and $\chi(\lambda)$ a lot compared with the non-turbulent magnetized envelopes. For large λ the polarization $p(\lambda)$ tends to zero much more rapidly than in the envelopes with only the regular magnetic field (see Figs. 2–5). We present asymptotic formulae for $p(\lambda)$ at large λ for various models of $\boldsymbol{B}(\boldsymbol{r})$ and $N_e(\boldsymbol{r})$ which can be used, in principle, to estimate the characteristic level of magnetic fluctuations $\langle B'^2 \rangle / B_0^2$ and the size of turbulent "cells"; however, this analysis requires the spectra $p(\lambda)$ and $\chi(\lambda)$.

The numerical calculations demonstrate that the observable polarization ($p \geq 0.01\%$) corresponds to the values $\delta_s \tau_{env} \leq 10^3$. Roughly, this means that $\lambda^2(\mu m) B_s(G) \leq 10^3$. The photons with energy 1 eV have the wavelength 1.24 μm. The photons with energy about (10–100) keV have wavelengths of $\approx 10^{-4}$ μm. Thus, the surface magnetic fields $B_s \leq 10^3$ G can produce the observable polarization in visible and infrared intervals of the scattered radiation wavelengths. The magnetic fields $B_s \approx (10^9-10^{11})$ G can be detected from the polarimetric X-ray and γ-ray observations.

The presented theory and the particular calculations can be used to interpret the observed polarimetric data from many cosmic objects possessing the magnetized envelopes and jets (quasars, active galactic nuclei, etc.).

References

Blaes, O. M. 2003, in Les Houches Session LXXVIII, 2002, Accretion discs, jets and high energy phenomena in astrophysics, ed. V. Beskin, et al. (N.Y.: Springer), 147

Brown, J. C., & McLean, L. S. 1977, A&A, 57, 141

Cherepashchuk, A. M. 2001, Usp. Fiz. Nauk, 171, 864 (Phys. Usp., 44, 821 (2001))

Chesneau, O., Wolf, S., & Domiciano de Souza, A. 2003, A&A, 410, 375

Dolginov, A. Z., Gnedin, Yu. N., & Silant'ev, N. A. 1995, Propagation and polarization of radiation in cosmic media (N. Y.: Gordon & Breach), 126

Dolginov, A. Z., & Silant'ev, N. A. 1974, Sov. Astron., 18, 289

Gradshteyn, I. S., & Ryzhik, I. M. 1994, Table of Integrals, Series and Products, 5-th edition (N.Y.: Academic Press), 439

Gnedin, Yu. N., & Silant'ev, N. A. 1980, SvA Lett., 6, 344

Gnedin, Yu. N., & Silant'ev, N. A. 1984, Ap&SS, 102, 375

Gnedin, Yu. N., & Silant'ev, N. A. 1997, Basic Mechanisms of Light Polarization in Cosmic Media, Astrophys. Space Phys. Rev., vol. 10 (New York: Gordon & Breach Publ.), 1

Gnedin, Yu. N., & Silant'ev, N. A. 2002, Astron. Lett., 28, 438

Gnedin, Yu. N., Silant'ev, N. A., Piotrovich, M. Yu., & Pogodin, M. A. 2005, Astron. Rep., 49, 179

Hartmann, L. 1983, In ed. J. O. Stenflo, Solar and stellar magnetic fields: origins and coronal effects (Dordrecht: Reidel), IAU Symp., 102, 419

Impey, C. D., Lawrence, C. R., & Tapia, S. 1991, ApJ, 375, 46

Ishwara-Chandra, C. H., Saikia, D. J., Kapahi, V. K., & McCarty 1998, Preprint No. 6198 (National Center for Radio Astrophysics)

Lamy, H., & Hutsemekers, D. 2000, A&AS, 142, 451

Landstreet, J. D. 1992, Astron. Ap. Rev., 4, 35

Leonard, D. C., Filipenko, A. V., Moran, E. C., Barth, A. J., & Matheson, T. 2000, ApJ, 536, 239

Long, K. S., Chanan, G. A., Ku, W. H.-M., & Novick, R. 1979, ApJ, 232, L107

Long, K. S., Chanan, G. A., & Novick, R. 1980, ApJ, 238, 710

Paatz, G., & Camenzind, M. 1996, A&A, 308, 77

Pentericci, L., van Reeven, W., Carilli, C. L., et al. 2000, A&AS, 145, 121

Pogodin, M. A. 1992, Pis'ma v Astr. Zh., 18, 442

Schmidt, G. D., & Hines, D. C. 1999, ApJ, 512, 125

Silant'ev, N. A. 2005, A&A, 433, 1117

Udompraset, P. S., Taylor, G. B., & Roberts, T. J. 1997, ApJ, 483, L9

Wills, B. J., Wills, D., Breger, M., Antonucci, R. R. J., & Barvainis, R. 1992, ApJ, 398, 454

Young, S., Hough, J. H., Efstathiou, A., et al. 1996, MNRAS, 281, 1206